Syarif_2020_IOP_Conf._Ser.__Mater._Sci._Eng._796_012057 NS

by Nirwan Syarif

Submission date: 25-Dec-2020 10:16PM (UTC+0700)
Submission ID: 1481231335
File name: Syarif_2020_IOP_Conf._Ser.__Mater._Sci._Eng._796_012057_NS.pdf (857.57K)
Word count: 3833
Character count: 19526

IOP Conference Series: Materials Science and Engineering

Preparing of Carbon Nanodots from Binchotan Carbon by Electrochemically Sonification and Dialysis

Preparing of Carbon Nanodots from Binchotan Carbon by Electrochemically Sonification and Dialysis

Nirwan Syarif [1, 2, 3*], Dedi Rohendi [1, 2, 3], Sri Haryati [4], Lee Chew Tin [5]
[1] Department of Chemistry, Universitas Sriwijaya, Indralaya, Sumsel, Indonesia
[2] Research Center of Excellence for Fuel Cell and Hydrogen
[3] National Center for Sustainable Transportation Technology, Bandung, Indonesia
[4] Department of Chemical Engineering, Universitas Sriwijaya, Indralaya, Sumsel
[5] Department of Bioprocess and Polymer Engineering, Universiti Teknologi Malaysia, Johor Bahru, Malaysia

E-mail: nsyarif@unsri.ac.id

Abstract. This paper reports the research of preparing an aqueous solution of binchotan carbon electrochemically and followed by its purification through sonification and dialysis. Binchotan rod and platinum plate were used as anode and cathode. The electrodes were placed on both sides of beaker glass that contained 200 ml of 14 M sulphuric acid, oxalic acid and phosphoric acid solutions as electrolytes, respectively. The potential between anode and cathode was 14 V. The solution was moved from beaker g[illegible] after 24 hours, filtered to produce a solid product for further examinations. The solid was washed with distilled water until pH 7, dried in 100℃ ovens. Two types of materials were examined, i.e. the product before and after the purification. The solid was then characterized by its morphology, crystallography, and surface functional groups by SEM, XRD, and FT- IR. The morphology of the binchotan after running the electro-oxidation process generally were aggregates and dots. Both shapes were reduced in size after purification. The diffractogram showed a significant change at 2Θ=14º- 44º meaning that the purification process changes the crystallography of carbon. The FTIR showed the presence of a functional group of aromatic, carboxylic, alkene, and alcohol on the surface of the carbon.

1. Introduction

Biomass carbonization basically produces carbon material containing a few functional groups because during pyrolysis the availability of oxygen in the reactor atmosphere reacts with carbon is very limited [1]. In the carbon surface modification, various types of functional groups are generated as the oxidation process is applied according to its power [2]. In practice, oxidation of carbon surfaces is done by reacting carbon sources with oxygen or oxygen-containing chemical compounds. Oxygen atoms that are inserted or added on the surface can also come from carbon raw materials that contain oxygen in their structures such as wood, sucrose, or phenol-formaldehyde resins, or oxidizing agents. The oxygen atom is cut off from the structure of its compound and diffuses and reacts with other carbon atoms on the surface of carbon forming a surface oxide or carbon oxide.

Surface oxides affect each other depending on interactions between adjacent functional groups. The overall interaction will affect carbon reactivity. The use of biomass-based carbon or biocarbon as a

* Corresponding author: nsyarif@unsri.ac.id

starting material in the oxidation process is more economically beneficial because such carbon already contains more or less functional groups on its surface [3].

One of the biocarbon has the potential to be developed for technical purposes is binchotan. Binchotan has the highest quality charcoal by burning for 14 days at high temperatures and cooling without using water. Binchotan has a high carbon content (> 95% by weight) with ~ 82% carbon hexagonal aromatic ring network arrangement [4], so it has the property to conduct electricity (conductor). Locally, the raw material of binchotan carbon is made from gelam wood, pelawan, eucalyptus, and other hardwoods. The woods are endemic crops of the island of Sumatra and some other islands of Indonesia [5]. Previous studies have shown several applications of binchotan as electrodes, both supercapacitors [6] and batteries. Furthermore, the conductive nature of binchotan is utilized to produce other functional carbon, i.e., carbon dots. The production is an analogy of the processes applied to graphite. Therefore, this work has never been done before, it is a novelty of this research.

The method commonly to produce carbon dot is electrochemical method [7]. The use of electrochemical methods for oxidation the carbon is more stable, safe, simple and can be expanded for mass production [8]. Electrochemical oxidation is carried out in simple equipment to produce uniform dots [9]. The electrochemical oxidation of graphite produces oxidized carbon with a high CO ratio and makes it possible to mass-produce the oxidized carbon (Ambrosi et al, 2015). The potential for electrochemical oxidation is 10 volts. At a voltage of 10 volts, the peeling process is slow and inefficient while a voltage greater than 10 volts makes the peeling rate take place so that the carbon particles will become thicker [10].

2. Materials and Methods

2.1. Oxidation of Binchotan

Binchotan rod and platinum plate were used as anode and cathode. Both electrodes were placed on both sides of the beaker glass that contained 200 mL of 14 M sulfuric acid solutions as electrolytes. The electrode was connected to the two poles of the power supply with two pieces of 2 mm diameter cable. The voltage applied to the anode and cathode was 14 volts for 24 hours operation. The same procedure was carried out for a solution of phosphoric acid and oxalic. At this stage in an aqueous solution of binchotan was obtained.

Purification of binchotan aqueous solution is carried out by sonification and dialysis. The solution was placed into the vial and rinsed in water. Sonification was done in an ultrasonic bath and operated for 2 hours. The ultrasonicated solution was removed from the vial and put into a dialysis tube. The solution and dialysis tube were into a beaker glass containing demineralized water. The water in the tube was stirred with a magnetic stirrer for 10 hours so that a high concentration of carbon dot solution in the tube was obtained and stored in the vial.

2.2. Material Characterizations

Binchotan aqueous solution before and after purification were moved from a vial, filtered to produce solid for further character examinations. The solid was washed with distilled water until pH 7 and was dried in 100℃ ovens. The solid was then characterized by its morphology, crystallography, and surface functional groups by SEM, XRD, and FT- IR. SEM measurement was in JEOL JSM 9390A. XRD patterns were produced from Shimadzu 7000 equipment, and FTIR spectroscopy was carried out by Shimadzu Prestige 21.

Acrylic glass plate 3 mm thick cut with a size of 4 cm x 1 cm, then washed with alcohol for 10 minutes in 50 mL beaker glass, then cleaned again with warm water. The acrylic glass was dried in the oven for 10 minutes at 100℃. Binchotan aqueous solution was taken 5 mL with 1 ml of permanent ink in a 50 ml beaker glass. Carbon was coated on the acrylic glass using a brush and dried in 100 °C oven for an hour. At this stage, a transparent electrode is produced which is ready to determine the electrical

conductivity and band gap values. The same procedure is also applied for carbon dot to an obtained electrode.

2.3. Performance Test

The transparent electrode is connected to the multimeter to measure the electrical resistivity (R) of carbon. The thickness of the glass before and after coated with the pasta was measured by using a digital caliper. The difference is the thickness of carbon to have d, and s is the measurement distance of the multimeter probes in the electrode. Therefore, K represents the conductivity. The resistivity of each glass is determined using the following mathematical formula:

$$\rho = R.\ s / d \quad (1)$$

$$K = 1 / \rho \quad (2)$$

The determination of the optical properties of biocarbon provides a transparent electrode. Spectrogram of the transparent electrode was obtained from UV-Vis spectrophotometer Shimadzu UV 7000 measurements. Binchotan transparent electrodes are inserted in the sample compartment to measure the transmittance at wavelengths of 400-800 nm in every the increasing of 20 nm. The optical band gap value is determined from the calculation of bandgap energy (bandgap) in a semiconductor material. Measurement with UV-Vis equipment will produce transmittance values in the maximum wavelength range. Electronic properties are determined based on the results of the bandgap energy calculation. Gap energy values can be obtained from the Tauc Plot method.

3. Results and Discussions

3.1. Material Characterisation

The SEM image presents a morphological interpretation of the prepared material using acids as electrolytes (figures 1). It represents the morphology of binchotan aqueous solutions produced by using 14 V of electrical potential. It can be shown that a part of the oxidized carbon is aggregated and the other is in the form of dots. In the foreground, the morphologies are dominated with aggregates while in the background are dots. A clear image of the dots that fill the solution can be seen in figure 2. The aggregates have a size range from 0.5 to 80 micron, and the dots have a size range from 40 to 150 nm. The dots tend to have regular morphology, inversely in two other electrolyte solutions, i.e. sulphate and phosphate (figure 1A and 1C). The same dot can be found in the oxidation results of polystyrene-graphite sintering [11]. The surface of binchotan aqueous oxalate (figure 1B) solution is rougher than the graphite oxidation results by pyrolysis which shows the surface of a circular hole formed. The same results can be found in binchotan aqueous sulphate solution.

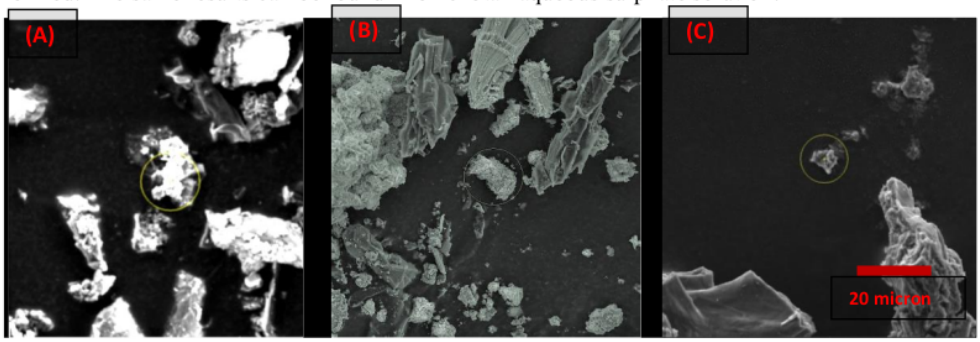

Figure 1. SEM images of binchotan aqueous solution contain electrolytes (A) sulphate (B) oxalate (c) phosphate.

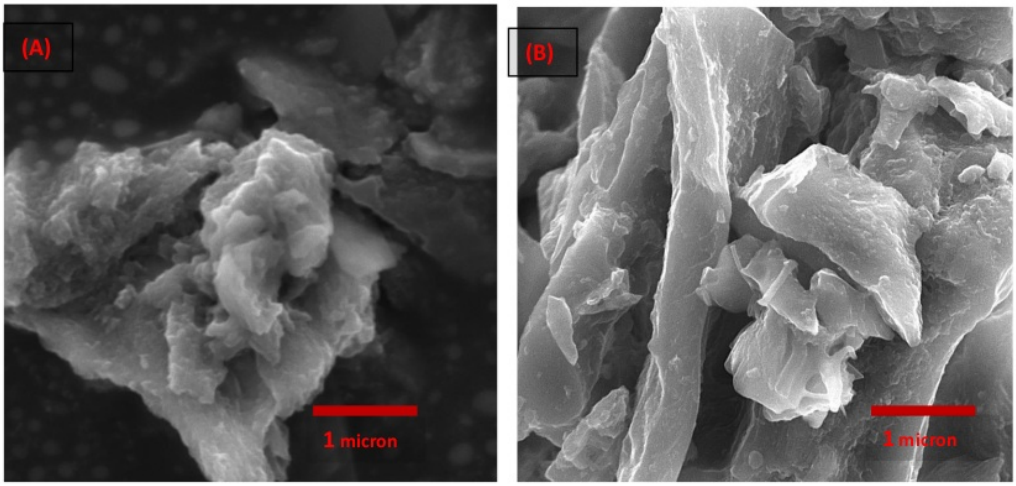

Figure 2. SEM image of binchotan aqueous solution contain (A) phosphate and (B) sulphate 14M, to show the dots in the carbon matrix.

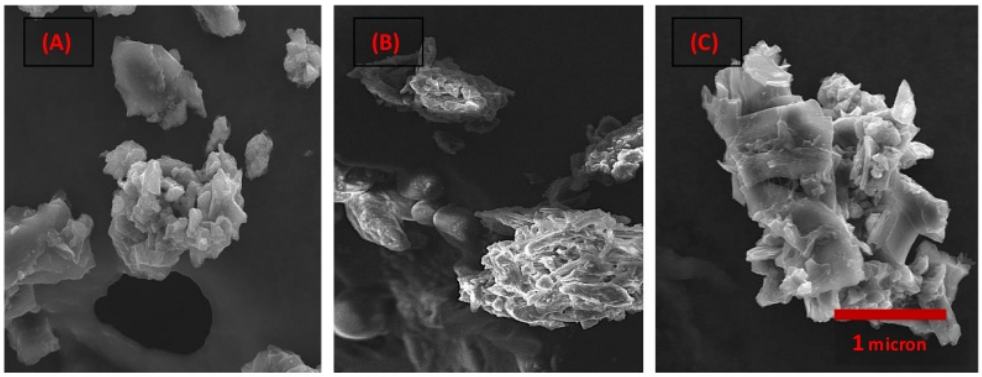

Figure 3. SEM images of binchotan aqueous solution after purification with electrolytes (A) sulphate (B) oxalate (c) phosphate.

Figure 1 (A) and (B) show the most eroded carbon surface is binchotan carbon which is oxidized electrochemically in sulphate and oxalate. The changes occur in the binchotan carbon surface after oxidation in sulphate solution, where the carbon surface becomes rougher (figure 2 B). This is because when oxidized using strong acid causes the reaction runs faster. The faster redox reaction the more oxidized binchotan carbon will also be rougher on its surface as explained in other papers [12]. The results of reduced carbon binchotan oxide show thinner aggregates on the surface of carbon that has been verified and has been observed with magnification 1000 times there is a form of carbon dot.

SEM image of binchotan aqueous with sulphate electrolyte after purification (Figure 3) shows aggregate sizes range from 80 to 2000 nm, with dots sizes range from 10 to 40 nm. Aggregates and dots size from the sulphate are the smallest compared to the other two solutions but relatively smooth (figure 3A). Figure 3B shows the aggregates and dots size of binchotan aqueous with sulphate electrolyte after purification that relatively the same as the sulphate with a more abrasive surface. Bigger aggregates dan dots can be found in binchotan – phosphate aqueous solution. Generally, the aggregates and dots become smaller after purification. The size reductions are caused by the

sonification process that induces flaking of the carbon layer in binchotan and reducing the surface of the carbon. The use of sonification also affects increasing temperature. The increase in temperature causes the bonds of oxygen and carbon to become weak so that hydrogen gas can easily push oxygen away from carbon, called the reduction process. The reduction in oxygen in the carbon causes loss of carbon mass [13].

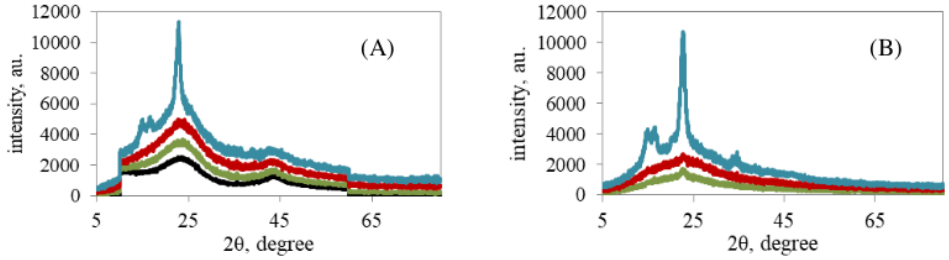

Figure 4. Diffractogram of binchotan (black line) and binchotan aqueous solution contain electrolytes sulphate (blue line), oxalate (red line), phosphate (green line); (A) before and (B) after purification.

The results using X-ray measurement can be seen in Figure 4. The diffractograms show that there is no significant change in carbon crystallography binchotan after oxidation using weak electrolytes (oxalate and phosphate). Inversely, crystallography of carbon is sharper after oxidation in sulphate, it can be shown that the peak in 2Θ = 23 is sharper with addition to peak in 2Θ = 14° that belong to graphene-like binchotan. The addition of acid as electrolytes is more likely to carry out the oxalate reaction with hydroxide from carbon so that more gas is formed, where the reaction occurs as follows (xxxx, 0000):

$$X^- + C\text{-}OH \longrightarrow HOX + C^+ + e^-$$

$$(COOH)_2 + XOH \longrightarrow 2CO_2 + H_2O + HX$$

Where X is an anion that is in an electrolyte solution. Therefore, the addition of HX will increase the production of oxidative products, in this case, HX is carbon. At the same time, some of the acids decrease with an increase in the initial concentration of acid. This causes an increase in the amount of oxalic acid needed for the amount of OX^- which is higher for oxidation. Conversely, higher concentrations of acid can reduce the diffusivity of the ions from the mass of the solution to the surface of the electrode and consequently reduce the rate of oxalic acid removal (Alhamed et al, 2016). In electrochemical oxidation, three types of acids, hydroxyl and carboxylic functional groups are formed. Both functional groups have the ability to form bonds between layers of carbon in addition to the electron cloud from C = C conjugated to the carbon layer. This is because the existence of functional groups in sulphate is relatively lower than weak electrolyte (oxalate and phosphate). The decrease in the number of functional groups increases the mobility of the carbon layer. This increase in carbon mobility provides greater opportunities for formation in carbon crystallites. The increasing size in carbon crystallites was detected by the presence of sharp peaks in the diffractogram [14].

The results of the purification of carbon binchotan oxide carried out using ultrasonic waves which are shows in the diffractograms Figure 4B. In addition, the reduction of shows the presence of a new diffraction peak, which is around the region of 2Θ = 35º. This peak comes from diffraction by silica/alumina [15]. This is because, in addition to reduction, the carbon surface treated by the ultrasonic method also exfoliates the carbon so that the presence of smaller particles begins to appear. This causes no significant changes in binchotan aqueous solution after purification as shown in figure 4B.

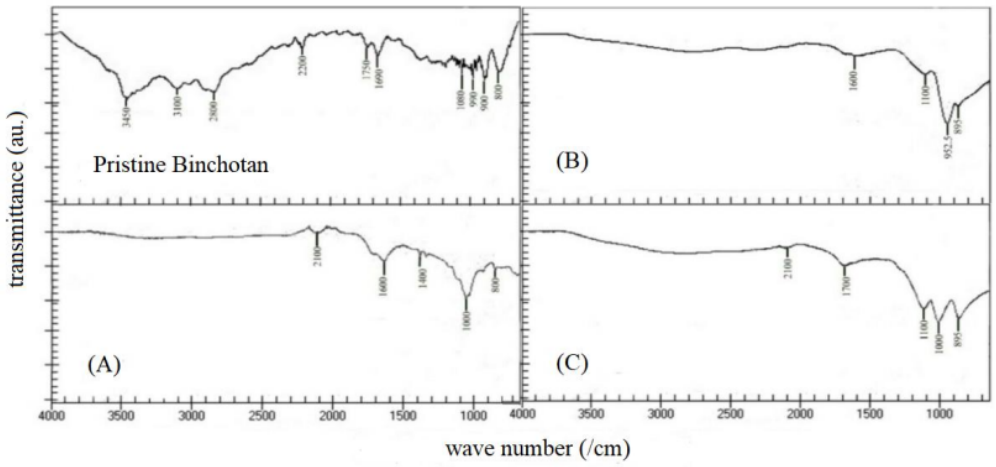

Figure 5. FTIR Spectrogram of prinstine binchotan and binchotan aqueous solution contain electrolytes (A) sulphate, (B) oxalate, (C) phosphate before purification.

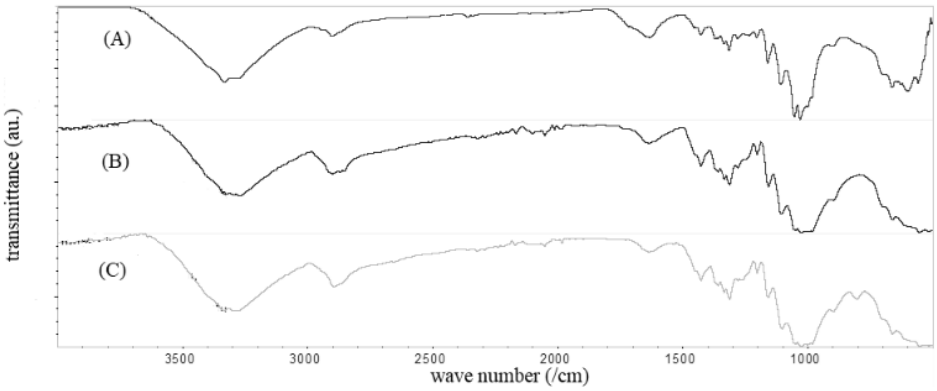

Figure 6. FTIR Spectrogram of pristine binchotan and binchotan aqueous solution contain electrolytes (A) sulphate, (B) oxalate, (C) phosphate after purification.

Analyses of FTIR provide more insight on the functional group of binchotan aqueous solution in electrolytes before purification (Figure 5). In general, FTIR spectras show that all binchotan aqueous solution have absorption at 3450 cm $^{-1}$ for CO in alcohol, 3100 cm^{-1} for CH in aromatic, 2800 cm^{-1} for CH in alkane, 2200 cm^{-1} for C≡C, 1750 cm^{-1} - 1690 cm^{-1} for C = O in carboxylic acid, and 1080 cm $^{-1}$ - 800 cm $^{-1}$ for C = C. FTIR sulphate (Figure 5A) spectra showed several absorption areas including at 2100 cm $^{-1}$ for C≡C alkaline functional groups, 1600 cm -1 for C = C aromatic functional groups, 1400 cm $^{-1}$ for CO alcohol functional groups, and 1000 cm^{-1} – 800 cm^{-1} for the alkene C = C. The FTIR spectra of the oxalate (Figure 5B) shows the absorption at 1600 cm -1 for the aromatic functional group C = C and 1100 cm^{-1} – 852.5 cm^{-1} for the alkene C = C functional group. The FTIR (Figure 5C) for the phosphate shows the peak at 2100 cm^{-1} for the C≡C alkaline functional group, 1700 cm $^{-1}$ for the carboxylic acid C = O function group, and 1100 cm^{-1} – 895 cm^{-1} for the C = C alkene group.

Analyses of FTIR provide more insight into the functional group of binchotan aqueous solution in electrolytes after purification (figure 6). The spectra for sulphate after purification in figure 6A shows

the peak, i.e. 3333.36 cm^{-1} for the OH alcohol function group, 2900.94 cm^{-1} for the alkane CH group, 1633. 61 cm^{-1} for the alkene functional group C = C, 1427, 75 cm^{-1} for the alkane functional group, 1315.31 cm^{-1} - 1030.56 cm^{-1} for the CO of alcohol functional group. FTIR spectra for oxalate after purification in figure 6B shows the absorption at an area of about 3400 cm -1 for OH functional groups, 2928.69 cm^{-1} for alkane CH functional groups, 1700 cm^{-1} for carboxylic acid functional groups C = O, 1137.06 cm^{-1} -1022.83 cm^{-1} for the CO alcohol functional group, and 867.65 cm^{-1} for the C = C alkene functional group. FTIR spectra for phosphate after purification in Figure 6C shows the presence of 2847.72 cm^{-1} alkanes CH functional groups, 2319.40 cm^{-1} for OH alcohol functional groups, 1621.05 cm^{-1} there were alkene functional groups C = C, 1104.45 cm^{-1} there is an alcohol functional group CO, and 971.98 cm^{-1} there is an alkene functional group C = C.

According to Quezada-Renteria, et.al [16], the change in functional groups is caused by the carbon oxidation occurred at 1.2 Volts forming hydroxyl groups on carbon. The oxidation strength is affected by the strength of the electrolyte. Where in this study the electrolyte strength series is $H_2SO_4 > H_3PO_4 > H_2C_2O_4$. The strength of oxidation helps the change in the hydroxyl group to the carbonyl group further to a carboxylate [17]. So that there is a large hydroxyl content in binchotan aqueous sulphate solution. In the reduction process, the ultrasonic treatment occurs in the formation of C-H bonds in the reduced carbon binchotan. This is due to the insertion of hydrogen atoms from water molecules into the carbon layer aided by ultrasonic waves. Besides, the O-H group from water is also bound to carbon as evidenced by the absorption peak in the FTIR spectra which tends to increase compared to the absorption peak in the O-H vibrational region.

4. Conclusions

Morphological interpretation of SEM images of the binchotan aqueous solution using acids as electrolytes shows that a part of the oxidized carbon is aggregated and the other is in the form of dots. In the foreground, the morphologies are dominated with aggregates while in the background are dots. SEM images show that the aggregates have a size range from 0.5 to 80 micron, and the dots have a size range from 40 to 150 nm for binchotan aqueous solution before purification and range from 80 to 2000 nm, with dots sizes range from 10 to 40 nm for binchotan aqueous solution after purification.

The results using X-ray show that there is no significant change in carbon crystallography binchotan after oxidation using weak electrolytes (oxalate and phosphate). Inversely, crystallography of carbon is more sharp after oxidation in sulphate, it can be shown that the peak in $2\Theta = 23$ is sharper with addition to peak in $2\Theta = 14^{o}$ that belong to graphene like binchotan. FTIR spectras show that all binchotan aqueous solution have absorption at 3450 cm^{-1} for CO in alcohol, 3100 cm^{-1} for CH in aromatic, 2800 cm^{-1} for CH in alkane, 2200 cm^{-1} for C≡C, 1750 cm^{-1} - 1690 cm^{-1} for C = O in carboxylic acid, and 1080 cm^{-1} - 800 cm^{-1} for C = C. The oxidation strength is affected by the strength of the electrolyte. Where in this study the electrolyte strength series is $H_2SO_4 > H_3PO_4 > H_2C_2O_4$.

Acknowledgments

The financial support for this research was provided by Universitas Sriwijaya. LPPM Universitas Sriwijaya is gratefully acknowledged for the award of 'hibah kompetitif' and 'hibah profesi' grant and supported by USAID through Sustainable Higher Education Research Alliances (SHERA) Program.

References

[1] Ertl P 2017 *J. Cheminformatics* **9**
[2] Chen J, Zhang Y, Zhang M, Yao B, Li Y, Huang L, Li C and Shi G 2016 *Chem. Sci.* **7** 1874–81
[3] Lim S, Yoon S-H, Mochida I and Chi J 2004 *J. Phys. Chem. B* **108** 1533–1536
[4] Chia C H, Joseph S D, Rawal A, Linser R, Hook J M and Munroe P 2014 *J. Anal. Appl. Pyrolysis* **109** 215–21
[5] Henri H, Hakim L and Batoro J 2017 *Biosaintifika J. Biol. Biol. Educ.* **9**
[6] Syarif N 2014 *Energy Procedia* **52** 18–25

[7] Ahirwar S, Mallick S and Bahadur D 2017 *ACS Omega* **2** 8343–53
[8] Zhang J and Yu S-H 2016 Mater. Today 19 382–93
[9] Fu Y, Gao G and Zhi J 2019 J. Mater. Chem. B 7 1494–502
[10] Yu Z, Tetard L, Zhai L and Thomas J 2015 Energy Env. Sci 8 702–30
[11] Rassaei L, Sillanpää M, Bonné M J and Marken F 2007 *Electroanalysis* **19** 1461–6
[12] Yi Y, Weinberg G, Prenzel M, Greiner M, Heumann S, Becker S and Schlögl R 2017 *Catal. Today* **295** 32–40
[13] Zhang G, Wen M, Wang S, Chen J and Wang J 2018 RSC Adv. 8 567–79
[14] Borah D, Satokawa S, Kato S and Kojima T 2008 Appl. Surf. Sci. 254 3049–56
[15] Syarif N, Ivandini Tribidasari and Wibowo W 2012 Int. Trans. J. Eng. Manag. Appl. Sci. Technol. 3 21 – 34
[16] Quezada-Renteria J A, Ania C O, Chazaro-Ruiz L F and Rangel-Mendez J R 2019 Carbon 149 722–32
[17] Bottani E J and Tascón J M D 2008 *Adsorption by carbons* (Amsterdam ; Boston ; London: Elsevier)

Syarif_2020_IOP_Conf._Ser.__Mater._Sci._Eng._796_012057 NS

ORIGINALITY REPORT

12%	9%	11%	10%
SIMILARITY INDEX	INTERNET SOURCES	PUBLICATIONS	STUDENT PAPERS

PRIMARY SOURCES

1	Submitted to Syiah Kuala University Student Paper	5%
2	M Miranda, R Suryanita, E Yuniarto. "Response structure analysis of prestressed box girder concrete bridge due to earthquake loads", IOP Conference Series: Materials Science and Engineering, 2020 Publication	1%
3	Nirwan Syarif, Dedi Rohendi, M. Ridho Prayogo. "Preparation of Kerosene Soot Carbon Electrode and Its Application in Lithium Ion Battery", 2019 6th International Conference on Electric Vehicular Technology (ICEVT), 2019 Publication	1%
4	repository.wima.ac.id Internet Source	1%
5	Submitted to Sriwijaya University Student Paper	1%
	academic.hep.com.cn	

6	Internet Source	1%
7	N F Syabania, W Sudarsono, D Rohendi, N Syarif. "Functionality Analysis of Carbon Nanosheet, Oxidized Carbon Nanosheet and Reduced Carbon Nanosheet Oxide by Using Fourier Transform Infra Red and Boehm Titration Method", Journal of Physics: Conference Series, 2018 Publication	<1%
8	Seongyop Lim, Seong-Ho Yoon, Isao Mochida, Jun-hwa Chi. "Surface Modification of Carbon Nanofiber with High Degree of Graphitization", The Journal of Physical Chemistry B, 2004 Publication	<1%
9	www.scopus.com Internet Source	<1%
10	www.theseus.fi Internet Source	<1%
11	Buryachenko, V.A.. "Multi-scale mechanics of nanocomposites including interface: Experimental and numerical investigation", Composites Science and Technology, 200512 Publication	<1%
12	Submitted to School of Business and Management ITB	<1%

Student Paper

Exclude quotes	Off	Exclude matches	Off
Exclude bibliography	On		